Properties of Mixtures of Silk Fibroin/ Syndiotactic-Rich Poly(vinyl Alcohol)

KAZUO YAMAURA, NORIYASU KURANUKI, MIYAKO SUZUKI, TETSUYA TANIGAMI, and SHUJI MATSUZAWA, *Faculty of Textile Science and Technology, Shinshu University, Tokida 3-15-1, Ueda-city, Nagano-prefecture 386, Japan*

Synopsis

The gelation of mixed solutions of silk fibroin (SF)/syndiotactic-rich poly(vinyl alcohol) (*s*-PVA), the thermal analysis of dry-gels, and the various properties of blend films were investigated. The rate of gelation of a mixed solution was lower than that of each SF or *s*-PVA solution of the same concentration. In the DSC thermograph of mixed dry-gel (SF/*s*-PVA = 2/8 – 8/2) 2 endothermic peaks corresponding to SF (at 288–299°C: decomposition) and *s*-PVA (at 233–241°C: melting) were found. Namely, microphase segregation took place. This was confirmed by optical and electron microscopes. The mechanical properties of blend films did not have additive properties. The degree of swelling in water of blend films was independent on water temperature or methanol treatment. The mechanochemical behaviors were barely observed by the pH exchange between pH 2 and 12 only under lower loads. The addition of SF into *s*-PVA films promoted the permeation of neutral salts.

INTRODUCTION

Recently the natural polymers with a compatibility to the living body have been noted as medical materials.[1] The applications of fibroin (SF) films as fungible of the skin and enzyme immobilized films, etc., are suggested.[2–4] SF films are, however, very brittle by themselves. PVA hydrogels are being studied in place of biological tissues[5] and used as a matrix for immobilization of microorganisms, enzymes, and heparin.[6–8] Syndiotactic-rich poly(vinyl alcohol) (*s*-PVA) has high water-resistance in comparison with commercial PVA (*a*-PVA).[9] We were able to make the blend films of *s*-PVA and SF from their mixed aqueous solutions. The blend films have a sea/island structure with moderate flexibility/strength. Therefore, they are considered to have wide application. Moreover, the blend films are worth noticing from the viewpoint of phase equilibrium between crystalline polymers. In this article, five properties (optical, thermal, swelling, mechanochemical, and permeation) of the blend films have been investigated.

EXPERIMENTAL

Preparation of Samples and Films

Regenerated aqueous silk (*Bombyx mori* L) was prepared by the way reported previously through dialysis of the lithium bromide solution.[10] The polymer con-

Journal of Applied Polymer Science, Vol. 41, 2409–2425 (1990)
 CCC 0021-8995/90/9-102409-17$04.00

centration was 1.39 g/dL. *s*-PVA was derived by the ammonolysis of poly(vinyl trifluoroacetate) (PVTFA) with diethylenetriamine. PVTFA was prepared by a bulk polymerization of vinyl trifluoroacetate (VTFA) at 60°C using benzoyl peroxide as an initiator. The degree of polymerization (DP) and the content of syndiotactic diad were 2720 and 56%, respectively. DP was determined from the intrinsic viscosity in benzene of the acetylated *s*-PVA using the formula $[\eta] = 8.91 \times 10^{-3} DP^{0.62}$ (dL·g^{-1}, 30°C).[11] The syndiotacticity of the *s*-PVA was determined from the infrared spectra.[12] *s*-PVA was dissolved in a sealed glass tube with water to gain the solution of the polymer concentration of 1.49 g/dL. Both aqueous solutions were carefully mixed at various mixture ratios avoiding flow-induced crystallization.[10,13] Blend films were obtained by casting the mixed aqueous solutions on glass plates at room temperature. The thickness of films used for the measurement of infrared (IR) spectra was 8–9 μm and for the measurement except IR spectra was 30–40 μm.

IR Spectra and Microscopy

The measurements of IR spectra were taken by using a Jasco A-302 infrared spectrophotometer for an untreated blend film (SF/*s*-PVA = 1/1, weight ratio), the blend film annealed at 200°C for 10 min, the blend film immersed in methanol, and the blend film immersed in methanol after annealing at 200°C for 10 min. The structure of films was observed by using a Nikon Optiphot-Pol polarizing microscope and a Jeol JSM-T220A scanning electron microscope.

Gelation and Thermal Analysis of Dry-Gel

Mixed solutions were held at 20°C and the gelation was investigated. After drying the gels, the thermal analysis was carried out by using a Rigaku-Denki DSC 8240B high-efficiency differential scanning calorimeter at a rate of 10°C/min.

Degree of Swelling

For the untreated film, the film annealed at 200°C, and the film immersed in methanol, the degree of swelling in water was measured at 30–80°C. The degree of swelling was estimated by dividing the equilibrium swollen length in water by the original length. The equivalent blend films were used. First, after the films were kept in water at 30°C for 30 min, the length and width of swollen films were measured by a cathetometer and the thickness was measured by a micrometer. Then, the films were kept at 40°C for 30 min and the degree of swelling was determined. Lastly, the films were kept at 80°C.

Tensile Test

Tensile tests were performed using a Shinko Model TOM/5 tensile tester at a crosshead speed of 10 mm/min and an original sample length of 20 mm at 25°C and under the relative humidity of 65%. The films were cut to a width of 2 mm. The measurement was carried out for the 5 films obtained under same conditions. The 4 kinds of films, i.e., unannealed, annealed at 200°C for 10 min, immersed in methanol for 1 h and annealed at 200°C for 10 min after immersion in methanol for 1 h, were used.

Mechanochemical Behavior

First, blend films (SF/*s*-PVA = 1/1, 1/2, weight ratio) were swollen in water at 30°C. The size of original films was ca. 30 mm × 2 mm × 30 μm. The weights of 1–7 g (in air) were held in water at the ends of swollen films and the equilibrium lengths were measured. Next, the swollen films were immersed in water of pH 2 and the length was measured as a function of time. After reaching to an equilibrium length, the swollen films were immersed in water of pH 12 and the length was measured as a function of time. After measuring the length under a load of 1 g, the swollen films were immersed in water at room temperature. The next day, the experiment was carried out again by using the swollen films at a load of 2 g, 3 g, . . . , and lastly 7 g (SF/*s*-PVA = 1/1) or 5 g (SF/*s*-PVA = 1/2).

Permeability of Neutral Salts

Cells consisting of 2 detachable parts made of glass were used for the permeability of neutral salts (NaCl, KCl, $MgCl_2$, and $MgSO_4$ conc.: 0.17, 0.134, 0.105, and 0.083 mol/L). An unannealed *s*-PVA casting film, the film annealed at 200°C, and the blended casting films (SF/*s*-PVA = 1/1, 1/2, and 1/3 weight ratio) were used. Their films were attached between 2 separated cells (cell I and cell II) and swollen in water at 30°C. Then, water was poured in cell II (volume: 90 mL) and aqueous solution of neutral salts was poured in cell I (266 mL). Immediately, the conductivity of the water side (cell II) was measured with time to estimate those concentrations.

RESULTS AND DISCUSSION

IR Spectra

Figure 1 shows the IR spectra for the various films. The absorptions at 1650, 1530, and 1235 cm^{-1} corresponding to random coils of silk fibroin are found for as-cast blend films. For the annealed films, their absorptions did not change, but the absorption at 1140 cm^{-1} corresponding to the crystallization of PVA became sharply. For the films treated by methanol, the absorption at 1650 cm^{-1} shifted to 1620 cm^{-1}. This shift is considered to be a random coil/β-form transition. For the film immersed in methanol after annealing, the shift to 1620 cm^{-1} was slight. This is due to the decrease in mobility of silk fibroin molecules induced by the crystallization of PVA molecules.

Gelation and Thermal Analysis

Figure 2 shows the relations between the gelation time at 20°C and the mixed ratio (volume ratio) of both solutions. The gelation time of 1.39 g/dL for regenerated aqueous silk was about 1 day and for 1.49 g/dL *s*-PVA aqueous solution it was within a day. The mixed untreated solution of mixture ratio of 7/3 (SF/*s*-PVA) had the largest gelation time. For the mixed annealed solution, the effect of annealing on the gelation time was remarkable in the solution of higher content of SF. Namely, the conformational change of silk fibroin molecules is considered to be induced by annealing the solution at high temperature.

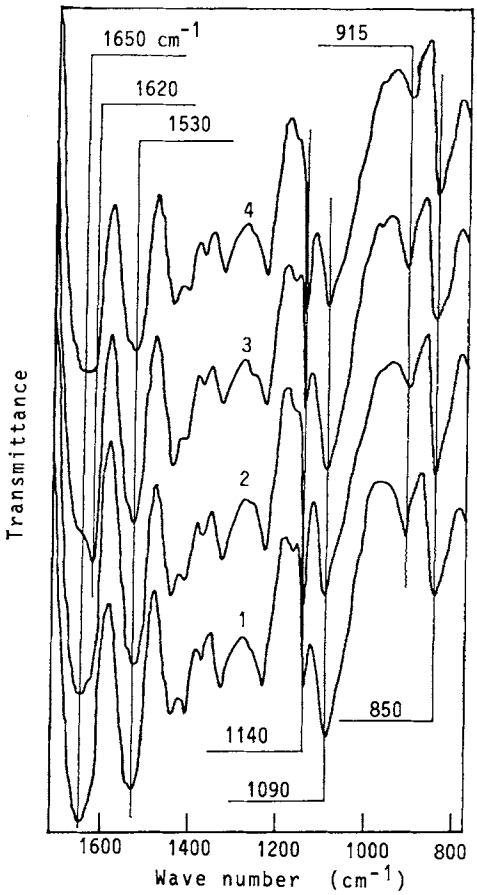

Fig. 1. IR spectra of mixed films of SF/*s*-PVA = 1/1. (1) as-cast film, (2) annealed at 200°C, (3) immersed in methanol, and (4) immersed in methanol after annealing at 200°C.

In the solution of lower SF content, *s*-PVA molecules contribute chiefly to gelation. The conformation change of PVA molecules is not induced by annealing since they have only random coil structure in the aqueous solution.

Figure 3 shows the DSC thermograph of dry-gels obtained from the mixed solutions in Figure 2. SF and *s*-PVA dry-gels had characteristic endothermic peaks at 288°C (decomposition of SF) and 241°C (melting point of PVA crystals), respectively, analogous to the results described previously.[14,15] In the blend dry-gel, the former and latter peaks shifted to high and low temperatures, respectively. The former peak was 299°C for the blend dry-gel of SF/*s*-PVA = 2/8 and the latter peak was 233°C for the blend dry-gel of SF/*s*-PVA = 8/2. As shown in Figure 3, both the peaks appeared in the DSC thermograph for the blend dry-gel of SF/*s*-PVA = 8/2 − 2/8. The decrement of melting temperature with a decrease in PVA content was considered from the decrease in the crystal size. The relation between the crystal size r (radius of sphere-like crystal) and melting temperature T_M of *s*-PVA crystals in blended films is shown in the following equation[16]

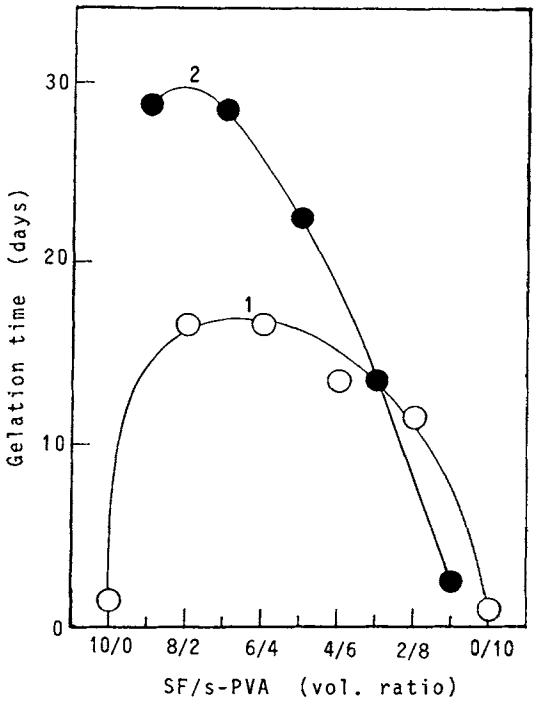

Fig. 2. Relations between the gelation time and the mixture ratio of SF/s-PVA solutions at room temperature. (1) untreated, (2) raised at a rate of 0.5°C/min from room temperature to 83°C.

$$T_M = T_m\left(1 - \frac{2\sigma}{r\Delta H_v}\right) \tag{1}$$

where T_m is the melting temperature of crystal of pure s-PVA polymer, σ is the surface free energy per unit area, ΔH_v is the heat of fusion per unit volume. In this paper, the crystal of PVA in the films was postulated as sphere and ΔH_v = 2000 cal·mol^{-1}, and T_m = 540 K were used.[17] As surface free energy, the mean surface energy of 4.1 erg·cm^{-2} for polyethylene was used.[18] The relation between T_M and the radius r is shown in Figure 4. The crystal size increased with the increment of T_M. In the blend dry-gel of SF/s-PVA = 9/1, however, the characteristic endothermic peak of s-PVA was not found at about 233°C. Moreover, in the blend dry-gel of SF/s-PVA = 1/9, the characteristic peaks of SF were not found at about 299°C. Namely, in both cases SF and s-PVA molecules are considered to mix each other satisfactorily.

In the blend films of SF/s-PVA = 1/1, microphase segregation was recognized by an optical microscope. It had a sea/island structure analogous to the very thin blend films (SF/s-PVA = 14/15) obtained by the frame method[19] and the islands had the diameter of ca. 1 μm. Both of the sea and island regions had no polarization. Figure 5 shows the scanning electron micrograph of as-cast films of SF/s-PVA = 1/2. The sea/island structure was recognized. The diameter of island was 1–5 μm. It was smaller than that of thin film obtained

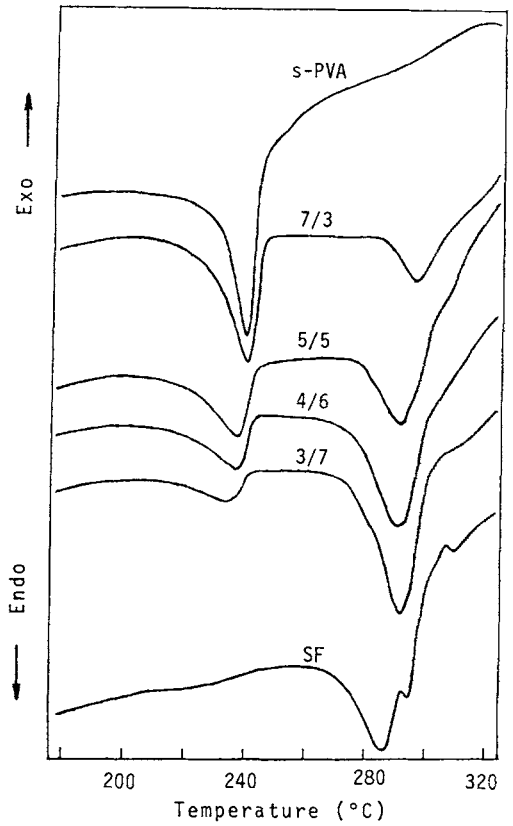

Fig. 3. DSC thermograph of dry-gel obtained in Fig. 2 for *s*-PVA, SF, and mixtures.

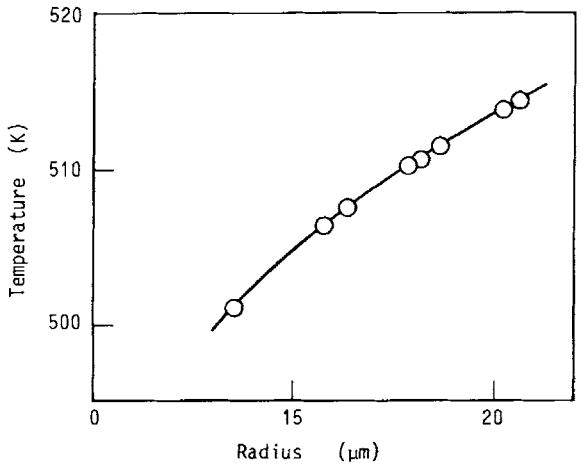

Fig. 4. Relations between the melting temperature of *s*-PVA in blended SF/*s*-PVA films and the radius of sea.

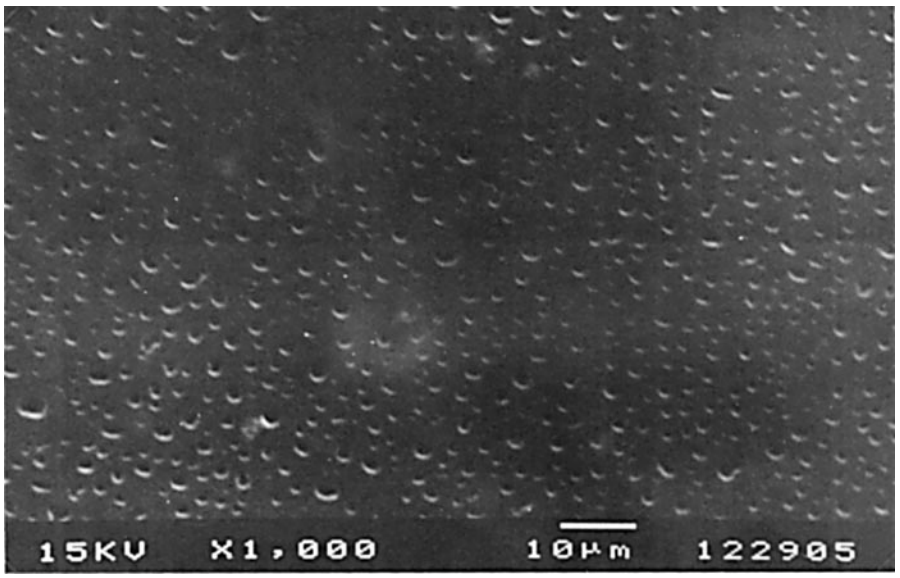

Fig. 5. Scanning electron micrograph of as-cast films of SF/*s*-PVA = 2/1.

by the frame method.[19] The aqueous solutions of SF, *s*-PVA, and blend SF/*s*-PVA gel easily. The gelation of blend SF/*s*-PVA is considered to be the phase equilibrium among SF crystals, *s*-PVA crystals, and water.

Swelling

Figure 6 shows the relation between the degree of swelling to the direction of length or thickness and the temperature for the equivalent blend films. The degree of swelling was roughly constant independent on water temperature. The swelling of *s*-PVA films were dependent on water temperature.[20] Therefore, the SF regions in the blend films are considered to interfere with the swelling of *s*-PVA regions. The solubility of blend films in water was very low (below 2%) even at 80°C. The degree of swelling to the direction of length was roughly constant independent of heat and methanol treatments, whereas to the direction of thickness, it was dependent on the treatments. The degree of swelling to the direction of thickness for the films annealed at 200°C was lower than that for the as-cast films or the films immersed in methanol. The effect of the conformational change of SF molecules for random coil to β-form on the degree of swelling to the direction of thickness was not recognized.

Young's Modulus

Figure 7 shows the relation between Young's modulus and the *s*-PVA content for the blended SF/*s*-PVA of films. The plot is not linear and had the minimum. If the rule of mixtures is established, Young's modulus of blend films E are shown by the following equation,

$$E = s_A E_A + s_B E_B \tag{2}$$

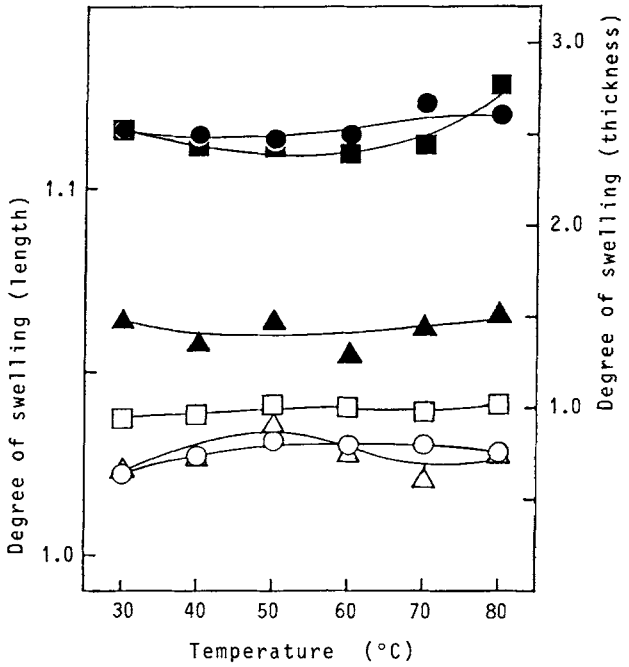

Fig. 6. Relations between the degree of swelling in water and the temperature for the equivalent mixed film. Length (○, △, □); thickness (●, ▲, ■). ○, ●: As-cast; △, ▲: annealed at 200°C; □, ■: immersed in methanol.

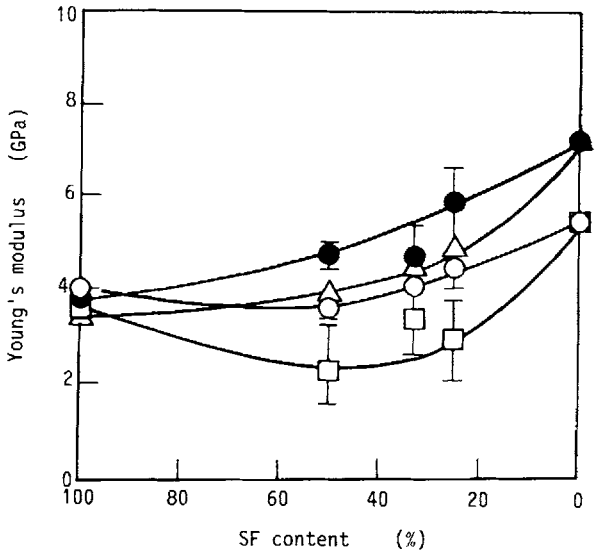

Fig. 7. Young's modulus plotted as a function of *s*-PVA content for the films of blended SF/*s*-PVA. ○: untreated films; ●: films annealed at 200°C; □: films immersed in methanol; △: films immersed in methanol after annealing at 200°C.

where E_A and E_B are Young's moduli of films for A and B elements, respectively, s_A and s_B are the fraction of A and B elements in blended films, respectively. Young's modulus of blends deviated from eq. (2). As shown in Figure 5, the blend films of SF/*s*-PVA had the sea/island structure. For the materials with sea/island phase separation, the adhesion at the interface between sea and island is considered to influence the mechanical properties of blend SF/*s*-PVA films.

The mechanical properties of blend SF/*s*-PVA films were evaluated by the modified Kerner equation shown as follows[21]

$$\frac{E}{E_1} = \frac{1 + AB\phi_2}{1 - B\psi\phi_2} \tag{3}$$

where E and E_1 are Young's moduli of the composite and matrix, respectively, and ϕ_2 is the volume fraction of filler phase. A, B, and ψ are given by the following equations

$$A = \frac{7 - 5\nu_1}{8 - 10\nu_1} \tag{4}$$

$$B = \frac{(E_2/E_1) - 1}{(E_2/E_1) + A} \tag{5}$$

$$\psi = 1 + \left(\frac{1 - \phi_m}{\phi_m^2}\right)\phi_2 \tag{6}$$

where ν_1 is Poisson's ratio, E_2 is Young's modulus of filler, and ϕ_m is the maximum volumetric packing fraction. Figure 8 shows the relations between E and ϕ_2 at $\nu_1 = 0.5$ and $\phi_m = 0.75$ for untreated films, $\phi_m = 0.6$ for films annealed at 200°C, and $\phi_m = 0.45$ for films immersed in methanol, respectively. Namely, the fillers are spherical and pack highly at $\phi_m = 0.75$, randomly at $\phi_m = 0.6$,

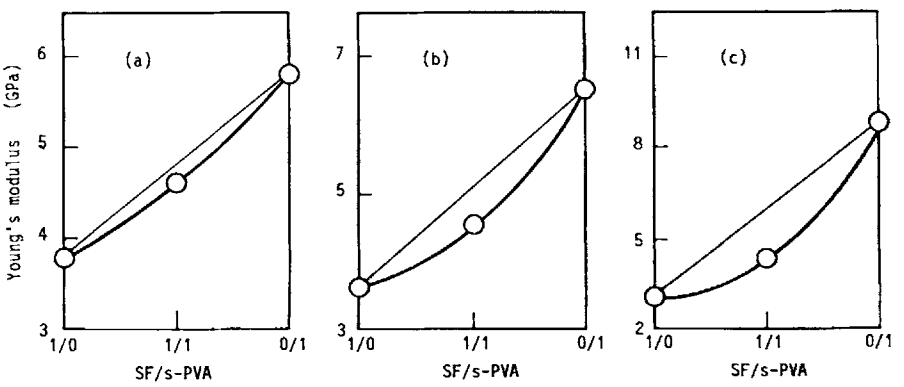

Fig. 8. Relations between Young's modulus obtained from eq. (3) and the volume fraction of filler phase. (a) $\phi_m = 0.75$ (untreated films), (b) $\phi_m = 0.6$ (films annealed at 200°C), (c): $\phi_m = 0.45$ (films immersed in methanol).

and as agglomerate at $\phi_m = 0.45$, respectively. The results were coincided with microscopic examination.

Mechanochemical Behaviors

Figure 9 shows the change of length with repeated cycles between pH 2 and 12 for the equivalent blend film. The blend film was swollen in water, contracted at pH 2, and elongated at pH 12. Remarkable elongation and contraction occurred. The repeated exchanges between pH 2 to 12 gave the contraction/elongation of sawtooth type. The swollen films reached to the equilibrium length after 30–40 min in each pH solution. Mechanochemical behaviors of synthetic polymers have been studied since 1950. Kuhn et al.[22] observed the mechanochemical behaviors for insoluble polyacrylic acid fiber crosslinked partially by PVA. Moreover, the crosslinked polymethacrylic acid fiber,[23] the glycerol-crosslinked poly-L-glutamic acid film,[24] etc., have been studied. The results are analogous to the results shown in Figure 9. Figure 10 shows the relations between the ratio of the equilibrium length in solution to original length and pH at various loads (in air, 1–7 g) for the equivalent mixed films. The mechanochemical behaviors lowered with the increase in load and disappeared under a load of 7 g. Namely, the load is higher than the contraction force of polymer chains. Figure 11 shows the change in mechanochemical behaviors induced by the load-exchange from 7 to 1 g. The mechanochemical behaviors appeared again. Figure 12 shows the relations between the ratio of the equilibrium length in solution to original length and pH for the blend film (SF/*s*-PVA = 1/2). Although larger elongation than that for the equivalent mixed film was observed, the mechanochemical behaviors already disappeared under a load of 5 g.

In the case of mechanochemical behaviors of blend SF/*s*-PVA films, the transition from chemical energy to mechanical energy is brought about by the transfer of protons. The changes of chemical energy to mechanical energy are given generally by the following equations[25]

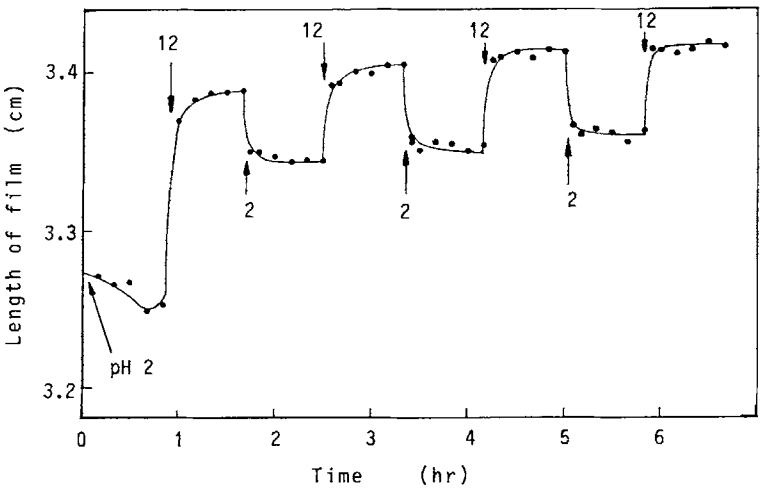

Fig. 9. Mechanochemical behavior of equivalent mixed SF/*s*-PVA films (30.3 mm × 2.0 mm × 30 μm) at 30°C. Load: 1*g* (in air).

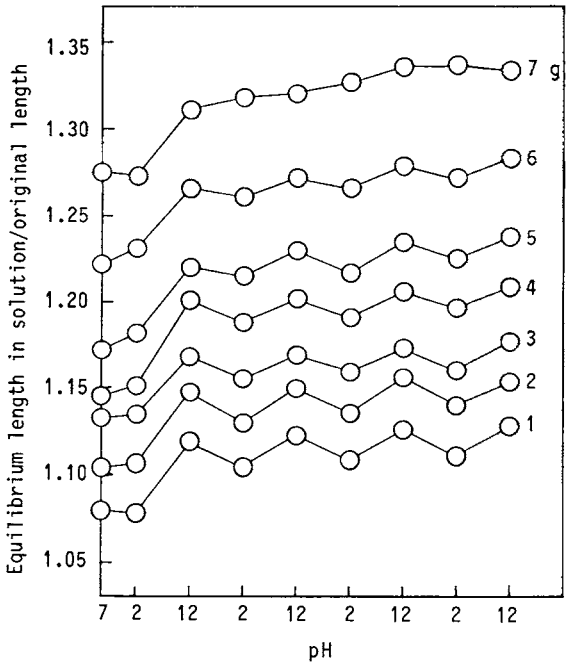

Fig. 10. Mechanochemical behaviors of equivalent mixed SF/*s*-PVA films under various loads at 30°C.

$$dW = dnRT \ln \frac{[\mathrm{H}]_{L2}}{[\mathrm{H}]_{L}} \tag{7}$$

$$dW = -fdl \tag{8}$$

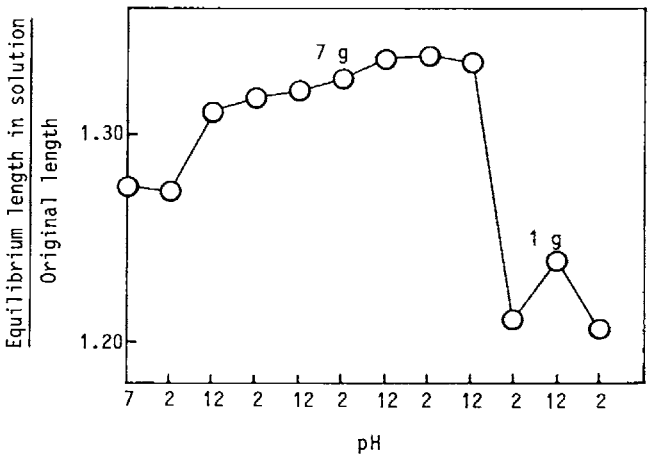

Fig. 11. The reappearance of mechanochemical behaviors of equivalent mixed SF/*s*-PVA film induced by the load-exchange from 7*g* to 1*g* at 30°C.

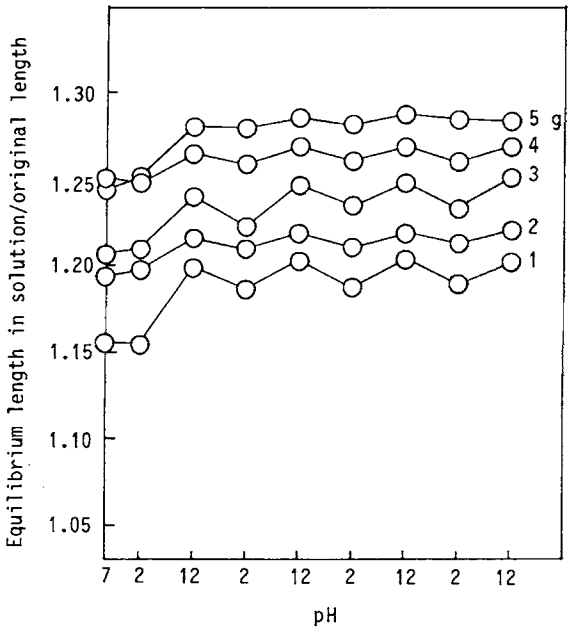

Fig. 12. Mechanochemical behaviors of mixed films (SF/*s*-PVA = 1/2) under various loads at 30°C.

where dn is the molar number of hydrogen-ion, R is the gas constant, T is the absolute temperature, $[H]_{L2}$ and $[H]_L$ are the concentrations of hydrogen-ion before and after drawing, f is the strength per unit area, and dl is the drawn-length. Equation (7) is shown by the following equation

$$dW = dnRT \ln \frac{a_{L2}}{a_L} \tag{9}$$

where a is the activity. Moreover, the molar number n of dissolved hydrogen-ions is given by the following equation,

$$n = \frac{xV\rho(\alpha + \beta)}{M} \tag{10}$$

where x is the volume fraction of SF, V is the volume of film, ρ is the density of SF (= 1.3), α is the fraction of aspartic acid in SF molecules, β is the fraction

TABLE I
The Molar Number per Cross Section (cm^2) of Hydrogen-Ion, n, Calculated from Eqs. (9) and (10)

Sample	From Eq. (9)	From Eq. (10)
SF/*s*-PVA = 1/1	3.9×10^{-7} mol	1.2×10^{-3} mol
1/2	2.3×10^{-7} mol	9.9×10^{-4} mol

of glutamic acid, and M is the molecular weight (= 66; the mean molecular weight of total amino acid residues in SF). The molar number of dissociated hydrogen-ions was calculated from eqs. (9) and (10) using the results at a load of 4*g* and shown in Table 1. Both values did not coincide. This is considered due to the parameters assumed and the presence of *s*-PVA. The maximum contraction force per unit area induced by mechanochemical action was estimated 3.0×10^9 dyne/cm^2 for SF/*s*-PVA = 1/1 film and 2.2×10^9 dyne/cm^2 for SF/*s*-PVA = 1/2 film.

Permeation of Neutral Salts

Figure 13 shows the conductivity change with time in water side under the permeation of sodium chloride through *s*-PVA or SF/*s*-PVA blend films for aqueous sodium chloride solution/water system. In any films, the conductivity increased steeply until 50 min and then slowly. The conductivity for blend films of SF/*s*-PVA = 1/2 was highest and that of as-cast blend films was higher than that of as-cast *s*-PVA film. Namely, SF molecules in the blend films are considered to play an important role in the permeation of sodium chloride. Figure 14 shows the relation between the concentration of permeant $MgSO_4$ and time for SF/*s*-PVA films with various blended ratios which is analogous to Figure 13. Figure 15 shows the relations between the concentration of per-

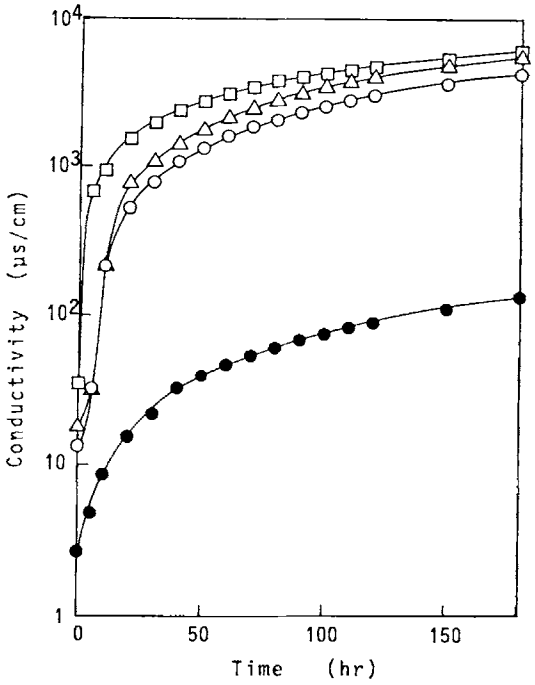

Fig. 13. Time-dependency of conductivity in water side by permeating sodium chloride through *s*-PVA or mixed SF/*s*-PVA films for aqueous sodium chloride solution/water system at 30°C. ○: As-cast *s*-PVA film; ●: *s*-PVA film annealed at 200°C; □: mixed films of SF/*s*-PVA = 1/2; △: mixed films of SF/*s*-PVA = 1/3.

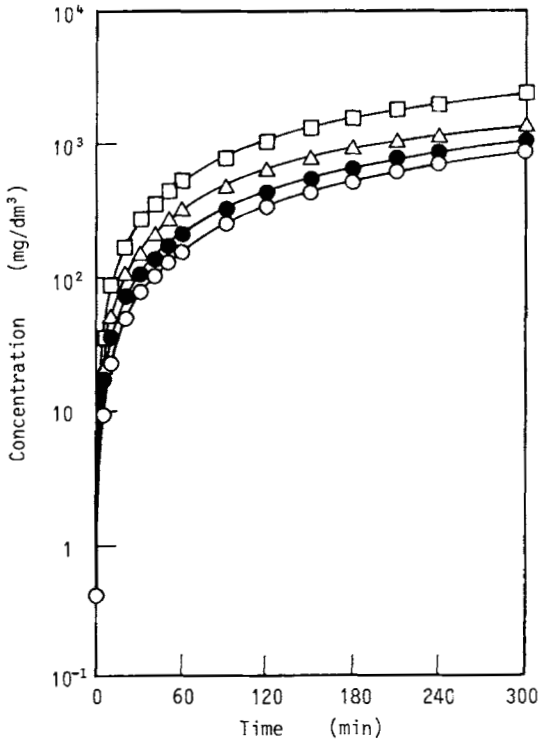

Fig. 14. Concentration of permeant $MgSO_4$ plotted as a function of time for mixed SF/*s*-PVA films (30°C). ○: *s*-PVA; ●: SF/*s*-PVA = 1/3; △: SF/*s*-PVA = 1/2; □: SF/*s*-PVA = 1/1.

meant salts and time for SF/*s*-PVA = 1/1 film. The permeation rate was KCl > $MgCl_2$ > $MgSO_4$, that is, it depended on ion size.

Ion permeation through membrane can be analyzed by Donnan's membrane equilibrium theory. In this article, the density of stationary electronic charge in blend film is low and the concentration of permeate salts is higher, that is, Donnan's membrane equilibrium is no longer viable. Therefore, we followed the method brought about by Sugiura[26] for the peremeation of KCl through SF film. The permeation rate of ion m is shown by the following equation[26]

$$m = \frac{v_2 dc_2}{dt} = K_m(f_1 c_1 - f_2 c_2) \tag{11}$$

where v_2 is the volume of permeant solution, c_1 and c_2 are the ion concentrations of permeate and permeant, f_1 and f_2 are the activity coefficients of permeate and permeant, t is time, and K_m is the apparent permeation constant. Moreover,

$$c_1 = c_1^0 - \left(\frac{v_2}{v_1}\right)c_2 \tag{12}$$

where c_1^0 is the initial concentration of permeate and v_1 is the volume of permeate. From eqs. (11) and (12), the following equation is obtained

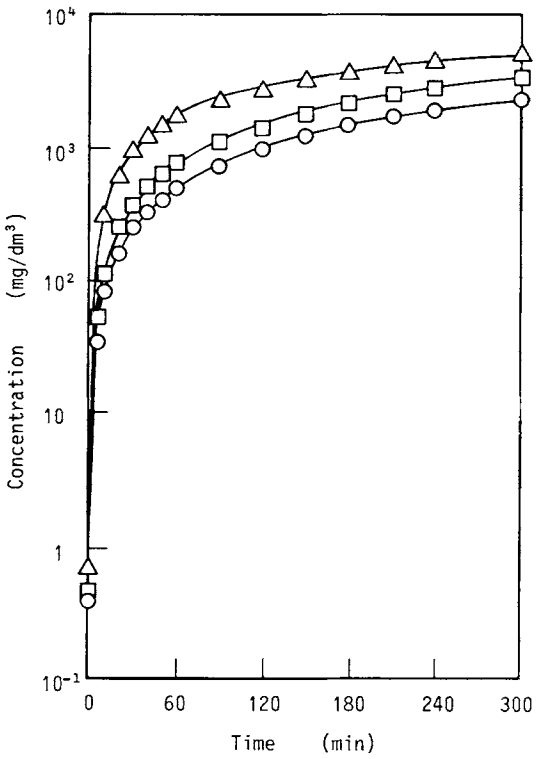

Fig. 15. Concentration of permeant salts plotted as a function of time for mixed films of SF/*s*-PVA = 1/1 (30°C). △: KCl; □: $MgCl_2$; ○: $MgSO_4$.

$$K_m = -\frac{v_2}{t}\left\{f_1\left(\frac{v_2}{v_1}\right) + f_2\right\}\ln\left\{\frac{f_1 c_1^0 - \left\{f_1\left(\frac{v_2}{v_1}\right) + f_2\right\}c_2}{f_1 c_1^0}\right\} \tag{13}$$

The permeation depended on the thickness d and area A of membrane. Therefore, the permeability was assessed by $K_m d/A$. Figure 16 shows the relations between $K_m d/A$ and the concentration of permeant. The permeability of ions is considered to be influenced by hydration radius of ions (K^+: 1.25 Å < Mg^{2+}: 3.43 Å, Cl^-: 1.20 Å < SO_4^{2-}: 1.90 Å).[27] For KCl permeation, $K_m d/A$ of SF film[26] and SF/*s*-PVA films was 5×10^{-7} and ca. 2×10^{-6} $cm^2\ sec^{-1}$, respectively. This considers that the degree of swelling of latter films was higher than that of the former.

CONCLUSION

1. In the blend films of SF/*s*-PVA = 2/8 − 8/2, microphase segregation was recognized.
2. In the mixed solution of high content of SF, the gelation was interfered by annealing.

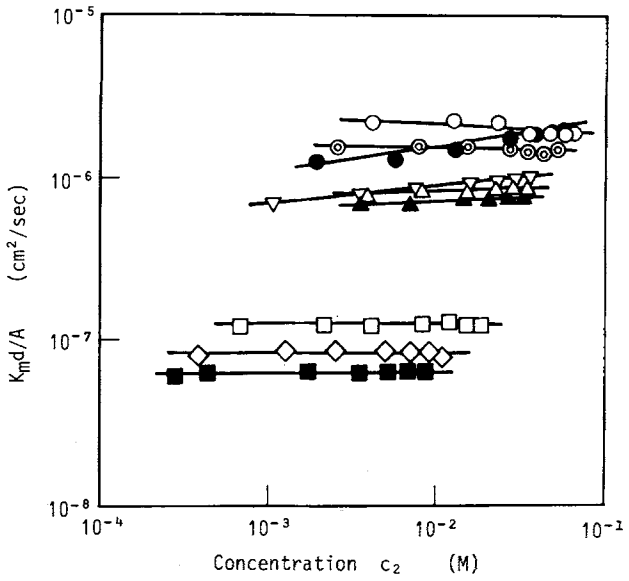

Fig. 16. Relations between $K_m d/A$ and c_2 for various neutral salts. KCl (○, ◎, ●); $MgCl_2$ (△, ▽, ▲); $MgSO_4$ (□, ◇, ■); SF/*s*-PVA = 1/1 (○, △, □); SF/*s*-PVA = 1/2 (◎, ▽, ◇); SF/*s*-PVA = 1/3 (●, ▲, ■).

3. In the blend films, the degree of swelling in water was independent on temperature and the methanol treatment.
4. The mechanical properties of blend films showed no additive property.
5. In the swollen blend films, the mechanochemical behaviors were barely induced by the repeated pH exchange between pH 2 and 12 only under lower loads.
6. The maximum contraction force per unit area induced by mechanochemical action was 2.2 − 3.0 × 10^9 dyne/cm^2 for SF/*s*-PVA = 1/2 − 1/1 films.
7. The addition of SF into *s*-PVA films promoted the permeation of neutral salts and the permeabilities of ions are influenced by the hydration radius of ions.

References

1. H. K. Kleiman, R. J. Klebe, and G. R. Martin, *J. Cell. Biol.*, **88,** 473 (1981).
2. M. Demura, T. Kuroo, and T. Asakura, *Polym. Preprints Jpn.*, **37,** 534 (1988).
3. J. Kanetake, T. Asakura, and M. Demura, *Polym. Preprints Jpn.*, **37,** 556 (1988).
4. T. Asakura, H. Yoshimizu, and M. Kakizaki, *Polym. Preprints Jpn.*, **37,** 1140 (1988).
5. M. Nambu, *Koubunshi Kakoh,* **32,** 523 (1983).
6. O. Ariga, H. Takagi, H. Nisizawa, and Y. Sano, *J. Ferment. Technol.*, **65,** 651 (1987).
7. A. Kozhukharova, N. Kirova, Y. Popova, K. Batsalova, and K. Kunchev. *Biotech. Bioeng.*, **32,** 245 (1988).
8. B. A. H. Smith and M. V. Sefton, *J. Biomedi. Mater. Res.*, **22,** 673 (1988).
9. K. Yamaura, A. Hayakawa, T. Tanigami, and S. Matsuzawa, *J. Appl. Polymer Sci.*, **35,** 1621 (1988).
10. K. Yamaura, Y. Okumura, and S. Matsuzawa, *J. Macromol. Sci. Phys.*, **B21** (1), 49 (1982).

11. A. Nakajima, *Kobunshi Kagaku,* **6,** 451 (1949).
12. S. Murahashi, S. Nozakura, M. Sumi, H. Yuki, and K. Hatada, *Kobunshi Kagaku,* **23,** 605 (1966).
13. K. Yamaura, M. Daimoh, T. Tanigami, and S. Matsuzawa, *J. Appl. Polym. Sci.,* **36,** 1707 (1988).
14. J. Magoshi, M. Mizuide, and Y. Magoshi, *J. Polym. Sci. Polym. Phys. Ed.,* **17,** 515 (1979).
15. M. Sumi, K. Matsumura, R. Ohno, S. Nozakura, and S. Murahashi, *Kobunshi Kagaku,* **24,** 606 (1967).
16. J. W. Gibbs, *Collected Works,* Longmans, Green & Co., New York, 1931, Vol. 1, pp. 55–372.
17. B. Hamada and A. Nakajima, *Kobunshi Kagaku,* **23,** 395 (1966).
18. L. Mandelkern, *Crystallization of Polymers,* McGraw-Hill, New York, 1964.
19. K. Yamaura, N. Kuranuki, K. Takeyama, M. Suzuki, T. Tanigami, and S. Matsuzawa, *Colloid Polym. Sci.,* to appear.
20. K. Yamaura, A. Hayakawa, T. Tanigami, and S. Matsuzawa, *J. Appl. Polym. Sci.,* **35,** 1621 (1988).
21. L. E. Nielsen, *J. Appl. Phys.,* **41,** 4626 (1979).
22. W. Kuhn, A. Katchalsky, B. Hargitay, and H. Eisenberg, *Nature,* **165,** 514 (1950).
23. A. Katchalsky and M. Zwick, *J. Polym. Sci.,* **16,** 221 (1955).
24. H. Noguchi and J. T. Yang, *Biopolym.,* **2,** 175 (1964).
25. W. Kuhn, *Makromol. Chem.,* **35,** 200 (1960).
26. M. Sugiura, *Nohgei Kagaku Kaishi,* **47,** 563 (1973).
27. J. Kieland, *J. Am. Chem. Soc.,* **59,** 1675 (1937).

Received October 23, 1989
Accepted January 20, 1990